Comparative activity of Platinum and Gold nanoparticles catalysts for Carbon monoxide oxidation

Jovine Emmanuel*

University of Dar es Salaam, Mkwawa University College of Education, Department of Chemistry, PO Box 2513 Iringa-Tanzania

ABSTRACT

The activity of Pt and Au nanoparticles catalysts over titania support for carbon monoxide oxidation was investigated. Pt and Au catalysts were synthesised by a high-throughput physical vapour deposition methodology (HT-PVD). A parallel thermographic screening methodology, which enabled the quantification of the activity of Pt and Au catalysts for CO oxidation reaction, was applied. A particle size effect in the catalytic activity of Pt and Au was observed, with the smallest particles exhibiting the highest activity. The activity of Pt and Au catalysts increased with temperature. Au catalyst displayed high activity at 80 °C, while Pt catalyst had higher activity at 170 °C. Although CO oxidation on Pt and Au catalysts is particle size-dependent, results show that Au nanoparticles catalyst exhibits the strongest particles size dependence as compared to Pt catalyst.

Keywords: Platinum; Gold; Titania; Nanoparticles; Particle Size
DOI: https://dx.doi.org/10.4314/ejst.v15i2.4

INTRODUCTION

The gas-phase CO oxidation reaction by O_2 on supported noble metal catalysts is crucial for both industrial and automotive pollution management (Bamwenda *et al.*, 1997). Over the decades, gold has been disregarded as a catalyst compared to platinum (Schubert *et al.*, 2001; Shaikhutdinov *et al.*, 2003; Risse *et al.*, 2008). The catalytic potential of small particles of gold was first discovered in the 1970s (Arenz *et al.*, 2006).

In 1973, it was shown that supported Au is catalytically active for olefin hydrogenation reaction (Chen and Goodman, 2008). In 1987, the work by Haruta and co-workers revealed that Au nanoparticles extensively dispersed on a high surface area metal oxides are catalytically active for the low-temperature carbon monoxide oxidation reaction (Haruta *et al.*, 1987). This discovery made Au

*Corresponding author: jovineemma2007@yahoo.co.uk

nanoparticles catalyst receive more attention in catalysis compared to bulk gold (Bamwenda *et al.*, 1997; Kung *et al.*, 2003; Comotti *et al.*, 2007). Studies have indicated that supported Au nanoparticles over the metal oxides support catalyse a series of reactions, including; selective hydrogenation, water gas shift, hydrochlorination and selective epoxidation (Cameron *et al.*, 2003). Therefore, there is a common interest in gold nanoparticles catalyst by researchers, and a lot of work that illuminates the uncommon catalytic property of gold has been so far reported (Schubert *et al.*, 2001; Lopez *et al.*, 2004; Remediakis *et al.*, 2005; Chen and Goodman, 2006; Molina *et al.*, 2009). In contrast, the Pt catalyst is the most useful heterogeneous metal catalyst that continues to enjoy enormous applications (Somorjai, 1994; Strasser *et al.*, 2003).

The catalytic activity of Pt was identified back in the early 1800s when Dobereiner used it to catalyse the reaction of H_2 and O_2 in his portable lamp (Somorjai, 1994). Thus, Pt is a widely studied heterogeneous catalyst that has experienced extensive use over the decades. Pt catalysts are applied in a series of reactions, such as the conversion of aliphatic straight-chain hydrocarbons to aromatic molecules and branched molecules (Somorjai, 1994). Pt catalyst is also applied in large-scale hydrogenation in the chemical and petroleum refining industries, and ammonia oxidation, which is an important reaction step in the fertilizer production process (Somorjai, 1994).

Crucially, Pt catalyst is applied for CO oxidation and unburnt hydrocarbons in automotive emissions management (Franceschetti *et al.*, 2003) and is the most extensively used catalyst in fuel cell technology (Kim and Jhi, 2011). Although Pt and Au are extensively used in catalysis, they are precious metals of high cost and less abundant thus, their application is limited. Their application at the atomic scale in heterogeneous catalysis is preferred to overcome the cost of using them as catalysts. This involves the dispersion of Pt and Au nanoparticles on high surface area metal oxides such as TiO_2, Al_2O_3, and Fe_2O_3, which in turn reduces the amount of Pt and Au in the catalysts (Somorjai, 1994).

Haruta (2003) has shown that small particles of Au supported on high surface area metal oxides catalyse CO oxidation reaction even at a temperature below 300 K compared to Pt which is catalytically more active than Au at a temperature higher than 500 K. Studies have indicated that the Au catalyst is four-fold more catalytically active at room temperature than Pt group metal catalysts that are commonly applied in CO oxidation reactions (Haruta, 2003; Haruta, 2004).

Findings show that Pt interacts strongly with CO, thus, hindering oxygen from adsorbing onto the surface of a catalyst (Schubert *et al.*, 2001; Molina *et al.*, 2009; Liu *et al.*, 2010). Thus, supported Pt catalysts are less active (Li *et al.*, 2008). Recent reports show that Pt nanoparticles supported on Fe_2O_3 have an

uncommonly high catalytic property for the gas-phase CO oxidation at low temperatures (Liu *et al.*, 2010). The activity of Pt nanoparticles catalyst has been linked to the ability of Fe_2O_3 to supply active oxygen during the reaction.

However, studies have shown that Pt nanoparticles below 5 nm over titania support either show low activity or no strong size dependence (Rashkeev *et al.*, 2007). Theoretical studies indicate that Pt nanoparticles of 1 nm or 2 nm sizes are catalytically more active (Dobrin, 2012). Reports from Kageyama and co-workers indicate that Pt nanoparticles of 2 nm sizes are more catalytically active than 3 nm and 5 nm sizes (Kageyama *et al.*, 2013).

Notwithstanding, several other studies (Goodman, 2003; Chen *et al.*, 2006; Hayden *et al.*, 2007) have indicated that supported Au nanoparticles catalyst in the size range of 1-5 nm are the most active particles for CO oxidation and that the Turn over Frequency (TOF) is strongly dependent on particle size. The report on an increase in specific mass activity of Au over titania with decreasing particle size is available (Herranz *et al.*, 2009). Although studies are available on Pt and Au dependence on particles size, there is no consensus concerning the activity trend with particle size for these systems.

This paper reports the comparative catalytic activity of Pt and Au nanoparticles catalysts supported on titania for CO oxidation at 80 ℃ and 170 ℃. An infrared thermographic technique that was first described in heterogeneous catalysis (Moates *et al.*, 1996) and later reviewed (Holzwarth *et al.*, 1998) was adopted to enable parallel screening of heterogeneous catalyst libraries synthesised by the HT-PVD method for CO oxidation. The results have revealed the ability of the HT-PVD method for controlled material synthesis.

MATERIAL AND METHODS

Synthesis of platinum and gold nanoparticles catalysts

A high-throughput combinatorial method based on HT-PVD discovered by Hayden *et al.* (2009) was applied to synthesise thin films of TiO_2 and TiO_2 supported Pt and Au nanoparticles catalysts. This method deposits thin films by the condensation of a vaporized material onto a substrate. The deposition chamber consisted of three electron gun (e-gun) evaporation sources (Temescal) and three Knudsen cell (K-cell) sources (DCA Instruments). The HT-PVD system operational base pressure was 1×10^{-10} mbar. Electron beam sources, E-gun 1 were used to evaporate Ti, and Pt and Au were evaporated from E-gun 3. Titania layers of approximately 200 nm were deposited onto a catalyst screening chip from

titanium (99.995%, Alfa Aesar metals) from E-gun 1 and oxygen (Air products, special gases, 99.999%) at a constant pressure of 9.7×10^{-6} Torr at 1 standard cubic centimetre per minute (sccm) oxygen flow rate and plasma source, $P_{rf} = 300$ W at a deposition rate of 4 Å/s with substrate kept at room temperature during film synthesis.

The thicknesses of titania layer deposits were controlled through deposition time, and sample thickness was subsequently established by calibration of deposition rates from AFM measurements. The AFM (Vecco Autoprobe M5) instrument was used in a contact mode with a silicon cantilever, a resonance frequency of 180 kHz, spring constant of 5 Nm^{-1} with an approximate tip (CSC17 probe, MikroMasch) curvature of 10 nm.

Platinum and gold nanoparticles characterization

For particle size characterization and distribution by TEM, the titanium dioxide layer, 15-25 nm thick, was deposited onto small carbon-coated copper TEM grids (Agar Scientific). These grids had TiO_2 deposited under similar deposition conditions as a catalyst screening chip. Pt and Au particles from Pt and Au sources (E-gun 3), were deposited onto a screening chip on which a titanium dioxide support material had been previously grown by using the HT-PVD method.

The deposition rate of 4 Å/s was established by depositing several thick layers from short to longer times, indicating that the thickness as established on contact masked samples by AFM was relative to the deposition time. The rate of Pt and Au deposition (0.15 Å/s) was established with the deposition of continuous Pt and Au thin films. Short deposition times (30 s – 360 s) were used to produce Pt and Au nanoparticles by nucleation and growth on titania substrates at 200 °C. For surface characterization of Pt and Au particles on the titania layer, Pt and Au particles were made onto Formvar® carbon-coated copper grids (Agar Scientific) coated with titania, 15-25 nm thick for transmission electron microscope (TEM) analysis.

Particle characterization was carried out using TEM before deposition onto the screening chip to ensure that particles were synthesized. The TEM images were acquired by using a Jeol 3010 instrument at a voltage of 300 kV, incorporating a Gatan CCD camera for recording the images. XPS measurements were undertaken in a UHV system incorporating a twin anode X-ray source (Mg Kα and Al Kα), and a VG Clam Single Channel XPS system analyser.

The depositions were carried out onto silicon nitride on silicon and on a 10 × 10 or 12 × 12 array micro-fabricated catalyst screening chip (450 μm silicon wafer thickness) on which a low-pressure chemical vapour deposited (LP-CVD) silicon

nitride membrane (300 nm and 600 nm) had been deposited. The screening chip had been back etched to produce individual membranes. The HT-PVD system was set up on a "wedge" deposition to synthesize various particle sizes distributions across the substrate.

A silicon screening chip with a dimension of 35 mm × 35 mm was made (450 mm thick silicon wafer) for infrared thermographic measurements, and an array of 10 x 10 silicon nitride membranes (1.5 mm × 1.5 mm) of thickness 600 nm were made through back etching of silicon to a layer of LP-CVD silicon nitride as described elsewhere (Emmanuel *et al.*, 2019). The membrane with the 200 nm of titania-supported catalyst was optically transparent. For the measurement of the temperature of the membrane, a graphitic carbon coating (200 nm) was sprayed on the back of the membrane giving an emissivity like that of a black body. A thin SiN membrane could support the catalyst with a small thermal mass and less thermal conductivity to the surrounding silicon chip so that heat produced by a reaction on the catalyst could consequently elevate the membrane's temperature.

Screening of platinum and gold catalysts for catalytic activity

The screening chip with the catalyst synthesised over the complete chip was placed on a heated sample holder with a heat shield which allowed the complete chip to be heated homogeneously to a base temperature for reaction of up to 250 °C. The sample holder was placed in a UHV chamber that had an IR transparent window (CaF_2), and the surface of the chip was imaged (50 mm focal length camera lens) by a thermal camera (Jade III, CEDIP) working in the spectral range of 3.6 – 5.1 μm with thermal sensitivity of 20 mK.

The spatial resolution of the camera was 320 × 240 pixels, and the complete 10 × 10 or 12 × 12 array was imaged to fill the detector. Reactions were undertaken in a turbomolecular pumped UHV chamber at a base pressure of 1×10^{-10} mbar, and the temperature response of the catalyst on the membrane for given power input (from an exothermic reaction) was calculated through finite element thermal modelling (Comsol Multiphisics®) (Emmanuel *et al.*, 2019).

The assumption was that the energy loss over the membrane would be through conduction through the membrane (together with the titania support and the graphite layer) to the supporting silicon chip. Radiative and convective losses were assumed to be zero thus, additional radiative and convective losses over a few degrees temperature over the base temperature of reaction would be expected to be very small. For CO oxidation reaction (ΔH = -283 $kJmol^{-1}$) and a pressure of 1×10^{-3} mbar, assuming every molecule reacts, the theoretical power was 2.289×10^{-4}

Js^{-1} mm^{-2} (Emmanuel *et al.*, 2019). This leads to a calculated temperature increase at the centre of the membrane, $\Delta T = 4$ °C. The calculated sensitivity of the chip enabled the establishment of TOF of reaction at the surface: the error associated with the absolute value of the TOF was estimated to be ca. +/- 30% mainly because of uncertainties in the thermal conductivity values for the composite membrane layer. A simulation of the temperature distribution across the 1.5 mm x 1.5 mm membrane had been previously reported (Emmanuel *et al.*, 2019).

RESULTS AND DISCUSSION

TEM images of Pt particles catalyst supported on titania are as described elsewhere (Hayden *et al.*, 2009). For Au on titania, TEM images were similar to that reported previously (Guerin *et al.*, 2006) in terms of particle growth. TEM images of Pt and Au nanoparticles catalysts supported on titania are indicated in Figures 1 and 2. TEM images enabled the establishment of particle size dependence of supported Pt and Au in relation to the equivalent coverage of Pt and Au deposited. In the Figures, Pt and Au particles are indicated in black against the substrate white background. At a short deposition time (30 seconds) in (a), the particles are smaller (black) clusters. However, as the deposition time increases, the particles grow in size since more Pt and Au are deposited as observed in the size of the particles in (b), (c), and (d), respectively, whose deposition times are 2, 3.5 and 5 minutes, respectively.

To determine the change in the particle size distribution after the CO oxidation reaction, as it was not possible to establish the distributions right on the screening chip by using TEM, XPS studies were undertaken before and after the reaction. Figures 3 and 4 present the XPS results for Pt and Au titania supported nanoparticles, respectively. In Figure 3, a shift in the Pt $4f_{7/2}$ peak of 0.7 eV for the 1.3 nm particles to higher binding energy (72.1 eV) was observed which increased to 0.9 eV at a peak position of 72.3 eV for the 4.5 nm particles followed by a dramatic drop to 0.5 eV at a peak position of 71.9 eV for the 6.6 nm particle size relative to bulk Pt $4f_{7/2}$ at 71.4 eV. The shift to higher binding energy for the smallest particles of Pt could be attributed to the final-state effect, in agreement with the available report (Liu *et al.*, 2014). However, for Au nanoparticles, a shift of about 0.42 eV to higher binding energy (84.42 eV) in the peak position was observed for 1.5 nm particles relative to bulk Au for the $4f_{7/2}$ core level at 84 eV. The shift decreased with increasing particle size to 0.1 eV for the 4.1 nm particles at 84.1 eV and it was 0.2 eV below bulk Au at 83.8 for the 5.8 nm particles, such a shift has been attributed to the final state effect (Guerin *et al.*, 2006).

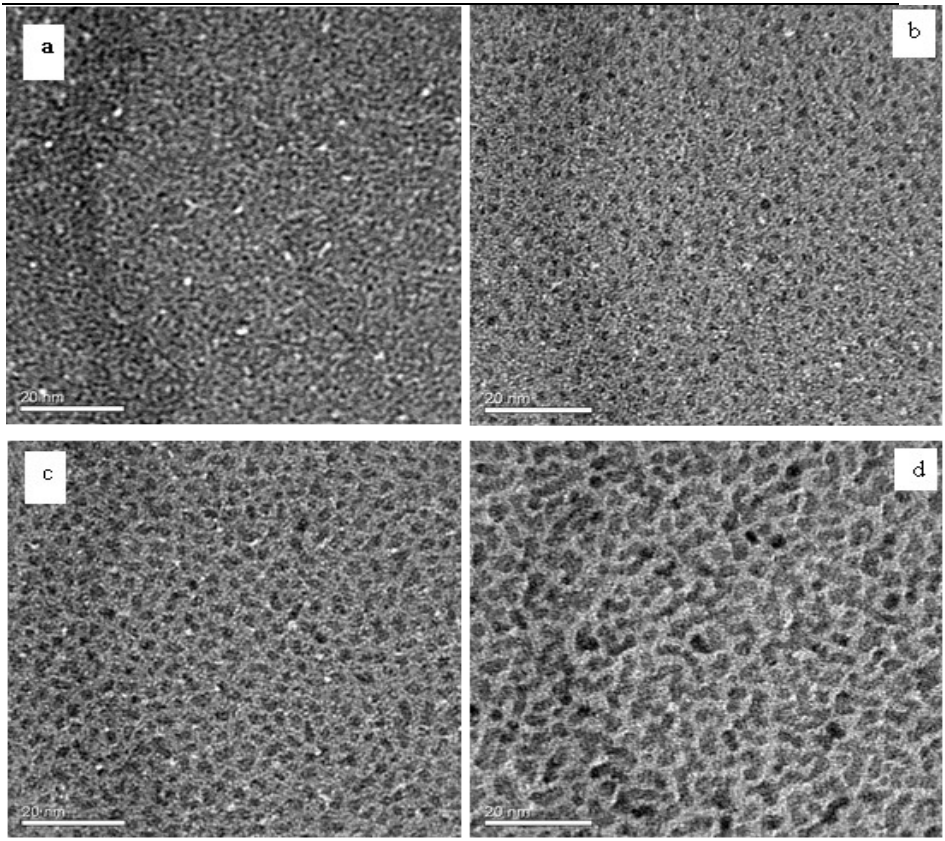

Figure 1. TEM images of Pt particles on titania at various deposition times, (a) 30 seconds, (b) 2 minutes, (c) 3.5 minutes and (d) 5 minutes with a mean particle sizes of (a) 1.6 nm, (b) 2.6 nm, (c) 4.9 nm and (d) 6.7 nm.

Generally, the study of the Pt and Au core level energies indicates a small but detectable shift in the binding energy. Studies show that the binding energy shifts depend on the species to which an atom is bonded and the binding energies shifts for the core level electrons can arise from either initial-state or final-state effects (Attard and Barnes, 1998; Kolasinski, 2002). Initial-state effects (chemical shift) are associated with chemical bonding which significantly influences the electronic configuration of an atom resulting in a significant shift in binding energy which in certain cases can be up to 10 eV (Attard and Barnes, 1998). Thus, atoms in a high oxidation state produce XPS peaks at high binding energy as compared to the same atom found in a low oxidation state (Kolasinski, 2002).

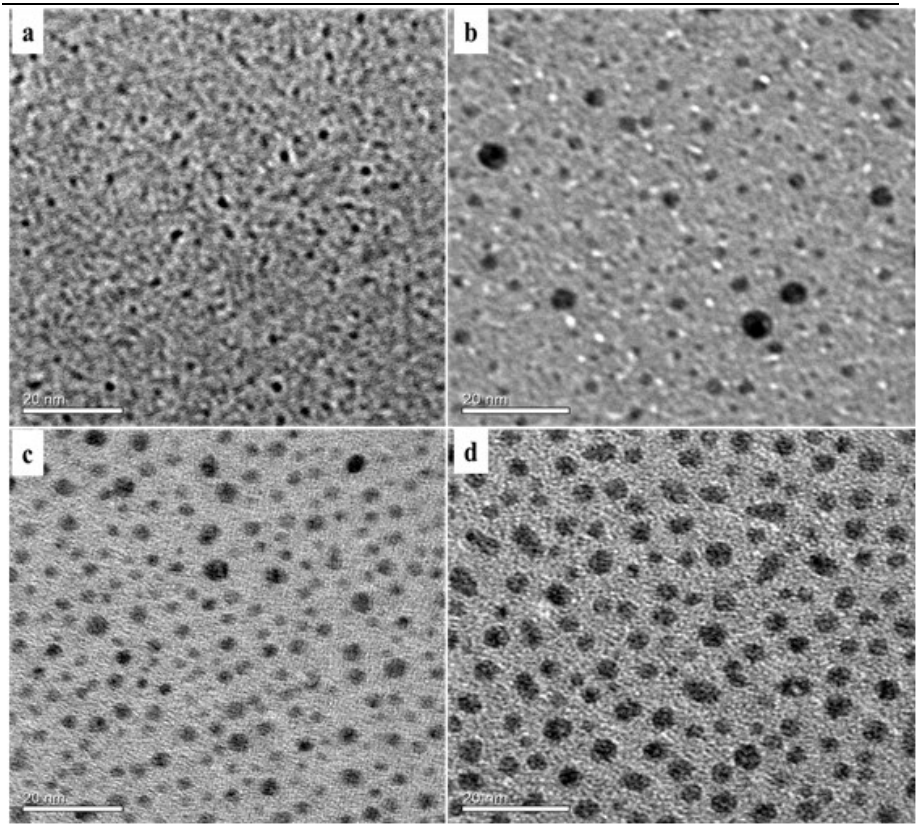

Figure 2. TEM images of Au particles on titania at various deposition times, (a) 30 seconds, (b) 2 minutes, (c) 3.5 minutes and (d) 5 minutes with a mean particle size of (a) 1.5 nm, (b) 2.8 nm, (c) 4.5 nm and (d) 5.8 nm.

Besides, the final-state effects are the result of the removal of an electron from an atom which corresponds to an ionic state creating a hole in place of the ejected photoelectron (Kolasinski, 2002). The effect of the binding energy shift as a result of the final-state is always a slight binding energy shift compared to that of the initial-state effect. Since the core level binding energy shift for Pt and Au nanoparticles observed in this study is smaller, typically less than 1 eV, these shifts are associated with the final state-effect, in agreement with the previous reports (Zhang *et al.*, 1997; Guerin *et al.*, 2006; Liu *et al.*, 2014). Figures 5 and 6 show the dependence of Pt $4f_{7/2}$ and Au $4f_{7/2}$ binding energy for Pt and Au particle size measured before and after reaction on Pt and Au supported catalysts on the screening chip.

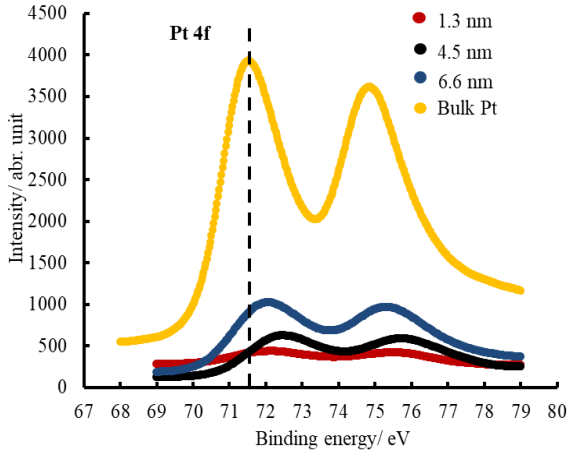

Figure 3. XPS spectra of the Pt (4f) core level for titania supported Pt particles with a mean diameter of 1.3 nm (red colour), 4.5 nm (black colour), 6.6 nm (blue colour), and bulk Pt (yellow colour).

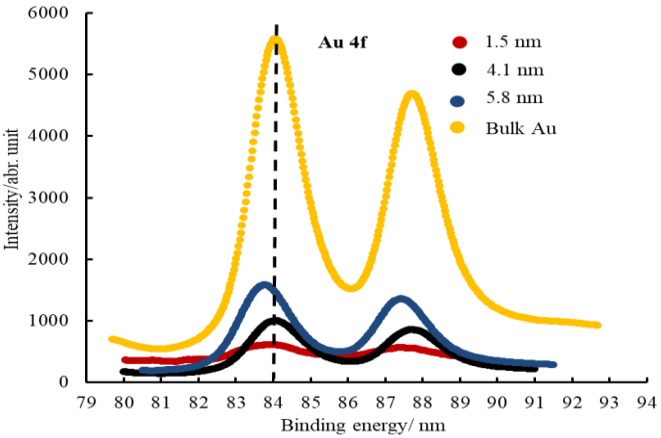

Figure 4**.** XPS spectra of the Au (4f) core level for titania supported Au particles of 1.5 (red colour), nm 4.1 nm (black colour), and 5.8 nm (blue colour) mean diameter and bulk Au (yellow colour).

Results revealed no major change in the binding energy shift of Pt and Au, implying that the particles remained stable throughout. However, the small difference in the binding energy shift for Pt and Au nanoparticles observed after the reaction could be attributed to the effect of experimental conditions on

nanoparticles. A consistent trend in the binding energy shift towards lower binding energy for Pt and Au nanoparticles after the reaction was observed and could be attributed to nanoparticles sintering/agglomeration except for the smallest particle size of Pt which indicates a sign of particle disintegration after the reaction. The increased intensity was observed with increasing particle size, indicating that Pt and Au particles grew in size as more Pt and Au were deposited. The measurements were made before and after the CO oxidation reaction had taken place. Within experimental error, the binding energy of Pt and Au remained the same for each particle size, implying that there was no major change in particle size during the reaction.

A catalyst library of 100 titania supported Pt and Au catalysts on the screening chip membranes was heated to a base reaction temperature in the HT-UHV chamber. The temperature variation across the chip at 300 ℃ was less than 2%. The temperature measurements approach for the membrane was as reported elsewhere (Emmanuel *et al.*, 2019).

The XPS spectra for the Ti 2p core level from TiO_2 upon which the Pt and Au particles were supported are shown in Figure 7. The Ti $2p_{3/2}$ peak in the titania film appears between 459.9 and 461 eV at higher binding energy than that of Ti metal at 454 eV. This is equivalent to the binding energy of Ti in TiO_2 (457.5 to 464.9 eV) which indicates that Ti is bonded to oxygen in the +4 oxidation state (Gao *et al.*, 2003).

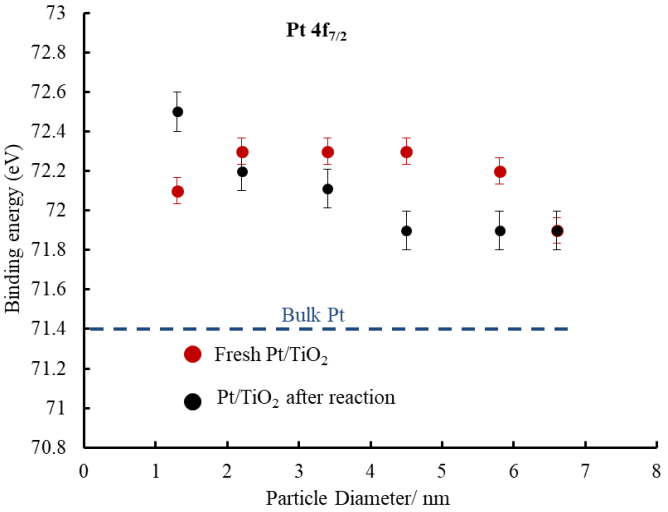

Figure 5. The binding energy and Pt particle size for the Pt 4f7/2 before and after the catalytic reaction.

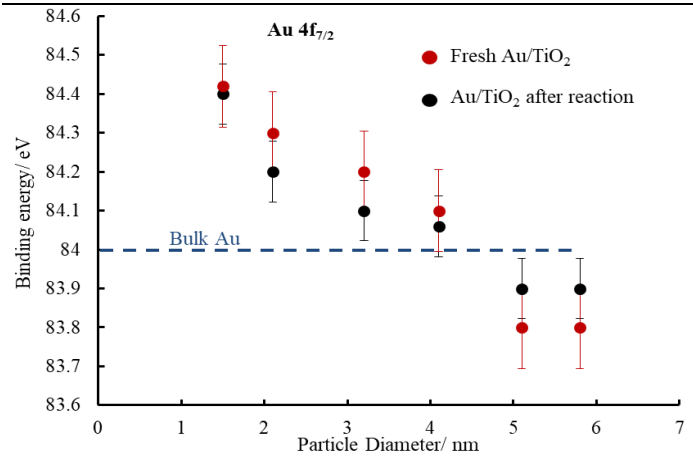

Figure 6. The binding energy and Au particle size for the Au $4f_{7/2}$ before and after the catalytic reaction.

Figure 7 (a) shows the Ti 2p XPS spectra on which Au particles were grown. A small change in Ti 2p intensity as a function of particle size is observed, perhaps Au particles exhibit 3D growth from the beginning of deposition which results in a smaller proportion of the substrate being covered. The binding energy of Ti $2p_{3/2}$ as a function of particle size (nm) is shown in Figure 7 (b). The Ti $2p_{3/2}$ peak appears at 458.4 eV and exhibits a small shift (0.1eV) to higher binding energy with no further shift with increasing particle size.

On the other hand, Figure 7 (c) indicates the Ti 2p spectra from TiO_2 upon which Pt particles were deposited. A constant Ti 2p intensity is observed as a function of particle size followed by a reduction in the Ti 2p intensity at a Pt particle size of 6.6 nm. The decline in the intensity at larger particle sizes of Pt can be attributed to the larger particles approaching each other to form aggregates thus, covering a large area of the substrate as reported elsewhere (Diebold, 2003). Because of the unchanging intensity, Pt particles exhibit a 3D growth mode from the beginning of the deposition. The XPS study on the effect of temperature on the growth mode of metal clusters has indicated that both Au and Pt particles exhibit 3D growth from the beginning at a deposition temperature of about 475 K (Zhang *et al.*, 1997). Since the Au and Pt particles in this study were deposited at 200 °C, 3D particle growth from the beginning of particle growth would be expected.

Figure 7 (d) presents the binding energy of Ti $2p_{3/2}$ as a function of particle size. The Ti $2p_{3/2}$ peak appears at 461 eV and slightly shifts by 0.1 eV to higher binding energy after which no further peak shift is observed with increasing particle size.

The peak shift to higher binding energy exhibited by Ti $2p_{3/2}$ where Au and Pt particles were supported may indicate that there is an interaction between Pt/Au and the substrate in agreement with previous studies (Meyer *et al.*, 2002; Jiang *et al.*, 2007).

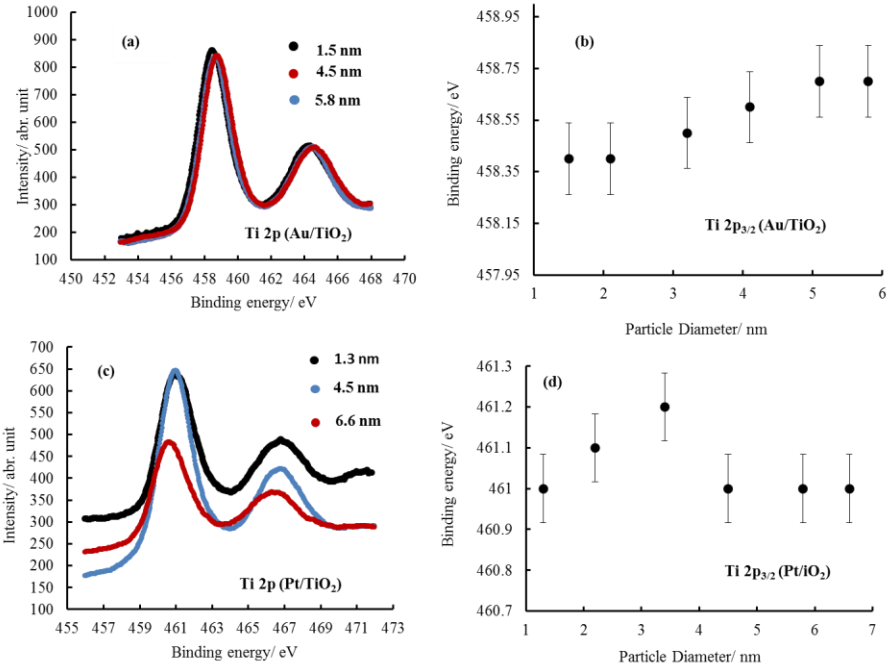

Figure 7. (a) XPS spectra of the Ti 2p core level for titania on which Au particles of various sizes were supported. (b) presents the binding energy of Ti $2p_{3/2}$ core level as a function of Au particle size. (c) Presents the XPS spectra of the Ti 2p core level of titania where Pt particles were supported and (d) is the binding energy of Ti $2p_{3/2}$ core level as a function of Pt particle size.

The XPS spectra of O1s core level for titania where Pt and Au particles of various sizes are supported are shown in Figure 8. The O1s peak on which Au particles were supported, Figure 8(a), appears at about 530 eV with a slight peak shift to higher binding energy at a constant intensity, the peak is at a position similar to the binding energy of O1s in TiO_2 as reported elsewhere (Gao *et al.*, 2003). The O1s peak where Pt particles were supported, Figure 8 (c), shifted to higher binding energy at about 532.5 eV compared to that of its Au counterpart with the observed decline in the peak intensity as Pt particle sizes grew larger which indicates that larger particles of Pt covered a larger area of the substrate.

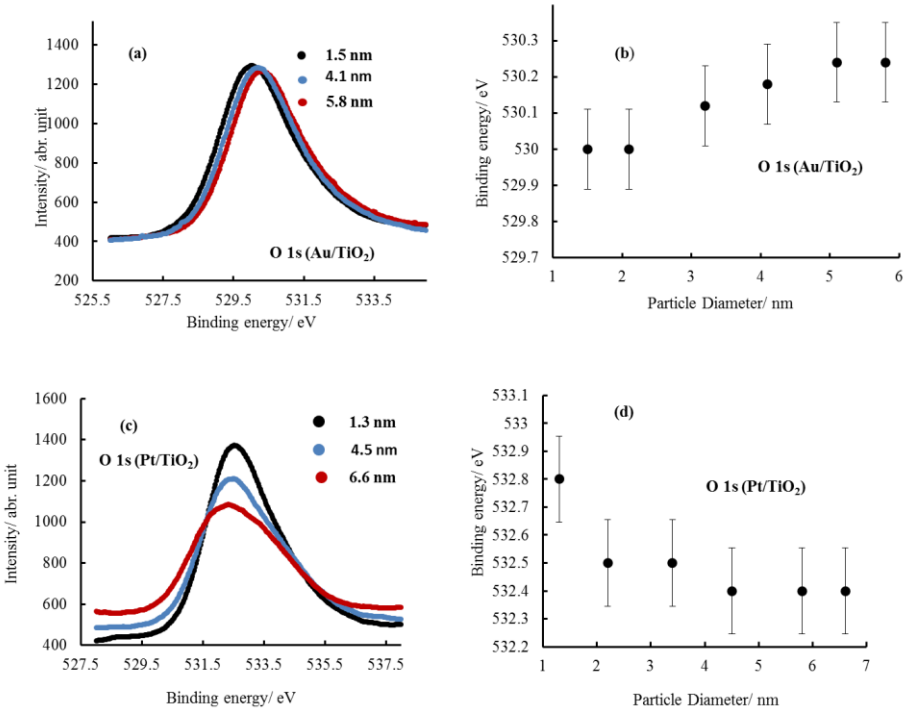

Figure 8. (a) XPS spectra of the O1s for titania where Au particles were supported. (b) presents the binding energy as a function of Au particle size. (c) Present the XPS spectra of O1s core level on which Pt particles were supported and (d) is the binding energy as a function of Pt particle size.

On Pt catalyst at a base temperature of 80 ℃, the total pressure of the gas mixture was 1×10^{-1} mbar with an O_2:CO ratio of 1:1 and 1.04×10^{-1} mbar with an O_2:CO ratio of 1:1 at 170 ℃. For Au catalyst at a base temperature of 80 ℃, the total pressure of the gas mixture was 8.4×10^{-2} mbar with an O_2: CO ratio of 1:1 and 6 x 10^{-2} mbar with an O_2: CO ratio of 1:1 at 170 ℃. The temperature was measured concurrently on all the catalysts integrated over a 5 minutes interval. The catalysts were synthesised in such a way that the particle sizes were constant across the rows, and varied in the columns of the screening chip. The change in temperature across a row of the same particle sizes was 0.2 ℃, far smaller than the changes in the columns and could be associated with a partial shielding of the gas flux at the edges of the sample by the holder. The temperature rise ΔT, on average, was used to compute the conversion rate of CO to CO_2 at the catalysts assuming the enthalpy of reaction was ΔH = -283 kJ mol^{-1} (Emmanuel *et al.*, 2019). The mass

and atoms of Pt at the surface of the particles per catalyst area were computed using TEM images, assuming hemispherical particles (Hayden *et al.*, 2009). This enabled the computation of TOF at Pt and Au surfaces. Figure 9 is a plot of TOFs for carbon monoxide oxidation on Pt at 80 ℃ and 170 ℃, the TOFs for CO oxidation on Au at 80 ℃ and 170 ℃ are presented in Figure 10. A monotonic increase in the TOFs for decreasing particle size was observed at these reaction conditions.

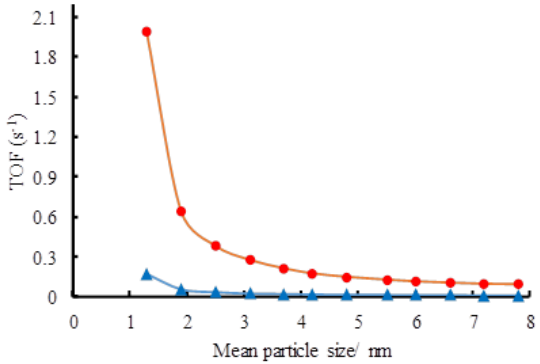

Figure 9. The TOF for carbon monoxide oxidation on Pt particles on titania. Results are shown for total pressures of 1.1×10^{-1} mbar with an O_2: CO ratio of 1:1 (blue triangles) at 80 ℃ and 1.04×10^{-1} mbar with an O_2:CO ratio of 1:1 (red circles) at 170 ℃.

Results show that the TOF of Au catalyst is higher than that of Pt catalyst at 80 ℃. The activity of 0.186 s^{-1} for Au catalyst was observed at 80 ℃ for Au particles size of 1.5 nm while Pt catalyst achieved the TOF of 0.171 s^{-1} at a similar temperature for Pt particle size of 1.3 nm. At 170 ℃, Pt catalyst attained the TOF of 1.991 s^{-1} for Pt particle size of 1.3 nm compared to 0.449 s^{-1} for Au of 1.5 nm. Studies have indicated that titania-supported Au nanoparticles are active for CO oxidation even at low temperatures as 300 K (Haruta *et al.*, 1997). The lower activity of Pt catalyst can be associated with the CO poisoning of the Pt catalyst surface at low temperature inhibiting O_2 adsorption and dissociation on the catalyst surface, an important process for the reaction to take place thus, retarding Pt catalyst activity. The previous report shows that an extremely active surface of Pt is witnessed at high reaction temperatures since at low reaction temperatures the CO inhibited regime is involved where the reaction is inhibited by adsorbed CO that hinders the adsorption and dissociation of O_2, resulting in the low catalytic activity of the Pt catalyst (Liu *et al.*, 2010).

While carbon monoxide oxidation on Pt and Au catalysts is particle size dependence, the most important point is the finding that Au catalysts possess a much stronger size-dependent effect than those of supported Pt catalysts.

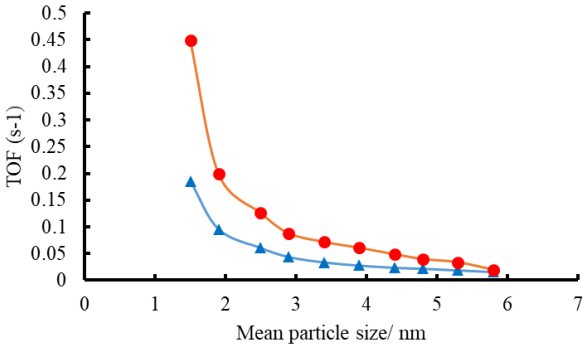

Figure 10. The TOF for carbon monoxide oxidation on Au particles on titania. Results are shown for total pressures of 8.4 × 10^{-2} mbar with an O_2:CO ratio of 1:1 (blue triangles) at 80 °C and 6 × 10^{-2} mbar with an O_2: CO ratio of 1:1 (red circles) at 170 °C.

For instance, the smallest particle of Pt achieved the maximum TOF of 0.25 s^{-1} at an O_2:CO ratio of 1:1, the total pressure of 0.72 × 10^{-2} mbar whereas that of Au had a maximum TOF of 0.45 at an O_2:CO ratio of 1:1, the total pressure of 0.6 × 10^{-2} mbar at 170 °C. This is because the bonding of CO or O_2 on Pt does not weaken the Pt-Pt bonds, which retards the activity as Pt would not benefit from perimeter sites compared to Au nanoparticles (Rashkeev *et al.*, 2007). Besides, Pt catalyst attained high activity at high temperatures as compared to Au catalysts, consistent with previous reports (Lin *et al.*, 1993; Herranz *et al.*, 2009). While there is no apparent consensus in the literature concerning the particle size effect for titania supported Pt nanoparticles catalyst, studies have demonstrated that the activity of titania supported Pt particles in the range between 1.1 nm and 10 nm for the CO oxidation reaction at various reaction temperatures increases with decreasing particle sizes (Li *et al.*, 2013). Besides, studies show that the catalytic activity of titania supported Au nanoparticles catalyst increases with decreasing particle size although there is no apparent consensus on the optimum particle size with the highest catalytic activity (Overbury *et al.*, 2006). Generally, there is an agreement that the activity of titania supported Pt and Au nanoparticles catalyst for CO oxidation reaction increases with the decrease of particle size. The rationale is that for particle size of diameter less than 10 nm, the relative number of kink sites, steps and corners increases exponentially with decreasing diameter. These under-coordinated surface atoms have a significantly different capability to interact with molecules from the gas phase.

CONCLUSION

The activity of Pt and Au model particles catalysts on titania with various particle sizes in the range between 1.3 nm to 7.8 nm and 1.5 nm to 5.8 nm, respectively, for carbon monoxide oxidation were measured on 100 or 120 catalysts simultaneously. XPS results have shown that there was no major change in the particle size of Pt and Au catalysts after the catalytic oxidation reaction. At the reaction conditions under which the reaction was studied, a monotonic increase in the TOF was observed with decreasing Pt and Au particle sizes. The activity was higher for Au catalyst compared to Pt at 80 ℃, with Pt catalyst displaying higher activity than Au at 170 ℃. The increase of activity for Pt at elevated temperature showed the dependence of carbon monoxide oxidation reaction on temperature, which agrees with previous reports on a similar system (Berlowitz *et al*., 1998; Li *et al.*, 2013). Results show that although carbon monoxide oxidation on Pt and Au catalysts on titania is particle size dependence, Au catalyst showed the strongest particle size dependence for CO oxidation compared to Pt catalyst.

ACKNOWLEDGEMENTS

The author honestly appreciates the significant contribution, advice and guidance, encouragement, and supervision roles of Professor Brian Hayden. The author also honourably acknowledges the financial support from the employer, Mkwawa University College of Education.

DECLARATION OF COMPETING INTEREST

The author has no conflicts of interest to declare.

REFERENCES

Arenz, M., Landman, U and Heiz, U. (2006). CO combustion on supported gold clusters. *ChemPhysChem* **7**(9): 1871–1879.

Attard, G and Barnes, C. (1998). Surfaces. Oxford University Press Inc, New York.

Bamwenda, G.R., Tsubota, S., Nakamura, T and Haruta, M. (1997). The influence of the preparation methods on the catalytic activity of platinum and gold supported on TiO_2 for CO oxidation. *Catalysis Letters* **44**(1): 83–87.

Berlowitz, P.J., Peden, C.H and Goodman, D.W. (1988). Kinetics of carbon monoxide oxidation on single-crystal palladium, platinum, and iridium. *The Journal of Physical Chemistry* **92**(18): 5213–5221.

Cameron, D., Holliday, R and Thompson, D. (2003). Gold's future role in fuel cell systems. *Journal of Power Sources* **118**(1-2): 298–303.

Chen, M., Cai, Y., Yan, Z and Goodman, D.W. (2006). On the origin of the unique properties of supported Au nanoparticles. *Journal of the American Chemical Society* **128**(19): 6341–6346.

Chen, M and Goodman, D.W. (2008). Catalytically active gold on ordered titania supports. *Chemical Society Reviews* **37**(9): 1860–1870.

Chen, M and Goodman, D.W. (2006). Catalytically active gold: From nanoparticles to ultrathin films. *Accounts of Chemical Research* **39**(10): 739–746.

Comotti, M., Weidenthaler, C., Li, W.C and Schüth, F. (2007). Comparison of gold supported catalysts obtained by using different allotropic forms of titanium dioxide. *Topics in Catalysis* **44**(1): 275–284.

Diebold, U. (2003). The surface science of titanium dioxide. *Surface Science Reports* **48**(5-8): 53–229.

Dobrin, S. (2012). CO oxidation on Pt nanoclusters, size and coverage effects: A density functional theory study. *Physical Chemistry Chemical Physics* **14**(35): 12122–12129.

Emmanuel, J., Hayden, B.E. and Saleh-Subaie, J. 2019. The particle size dependence of CO oxidation on model planar titania supported gold catalysts measured by parallel thermographic imaging. *Journal of Catalysis* **369**: 175–180.

Franceschetti, A., Pennycook, S.J and Pantelides, S.T. (2003). Oxygen chemisorption on Au nanoparticles. *Chemical Physics Letters* **374**(5-6): 471–475.

Gao, Y., Masuda, Y., Peng, Z., Yonezawa, T and Koumoto, K. (2003). Room temperature deposition of a TiO_2 thin film from aqueous peroxotitanate solution. *Journal of Materials Chemistry* **13**(3): 608–613.

Goodman, D.W. (2003). Model catalysts: from imagining to imaging a working surface. *Journal of Catalysis* **216**(1-2): 213–222.

Guerin, S and Hayden, B.E. (2006). Physical vapor deposition method for the high-throughput synthesis of solid-state material libraries. *Journal of Combinatorial Chemistry* **8**(1): 66–73.

Guerin, S., Hayden, B.E., Pletcher, D., Rendall, M.E., Suchsland, J.P and Williams, L.J. (2006). Combinatorial approach to the study of particle size effects in electrocatalysis: synthesis of supported gold nanoparticles. *Journal of Combinatorial Chemistry* **8**(5): 791–798.

Haruta, M. (2003). When gold is not noble: Catalysis by nanoparticles. *The Chemical Record* **3**(2): 75–87.

Haruta, M. (2004). Gold as a novel catalyst in the 21st century: Preparation, working mechanism and applications. *Gold Bulletin* **37**(1): 27–36.

Haruta, M., Kobayashi, T., Sano, H and Yamada, N. (1987). Novel gold catalysts for the oxidation of carbon monoxide at a temperature far below °C. *Chemistry Letters* **16**(2): 405–408.

Hayden, B.E., Pletcher, D and Suchsland, J.P. (2007). Enhanced activity for electrocatalytic oxidation of carbon monoxide on titania-supported gold nanoparticles. *Angewandte Chemie* **119**(19): 3600–3602.

Hayden, B.E., Pletcher, D., Suchsland, J.P and Williams, L.J. (2009). The influence of Pt particle size on the surface oxidation of titania supported platinum. *Physical Chemistry Chemical Physics* **11**(10): 1564–1570.

Herranz, T., Deng, X., Cabot, A., Alivisatos, P., Liu, Z., Soler-Illia, G and Salmeron, M. (2009). Reactivity of Au nanoparticles supported over SiO_2 and TiO_2 studied by ambient pressure photoelectron spectroscopy. *Catalysis Today* **143**(1-2): 158–166.

Holzwarth, A., Schmidt, H.W and Maier, W.F. (1998). Detection of catalytic activity in combinatorial libraries of heterogeneous catalysts by IR thermography. *Angewandte Chemie International Edition* **37**(19): 2644–2647.

Jiang, Z., Zhang, W., Jin, L., Yang, X., Xu, F., Zhu, J and Huang, W. (2007). Direct XPS evidence for charge transfer from a reduced rutile TiO_2 (110) surface to Au clusters. *The Journal of Physical Chemistry C* **111**(33): 12434–12439.

Kageyama, S., Sugano, Y., Hamaguchi, Y., Kugai, J., Ohkubo, Y., Seino, S., Nakagawa, T., Ichikawa, S and Yamamoto, T.A. (2013). Pt/TiO_2 composite nanoparticles synthesized by electron beam irradiation for preferential CO oxidation. *Materials Research Bulletin* **48**(4): 1347–1351.

Kolasinski, K.W. (2002). Surface science:Foundation of catalysis and nanoscience. John Wiley & Sons, University of London.

Kim, G and Jhi, S.H. (2011). Carbon monoxide-tolerant platinum nanoparticle catalysts on defect-engineered graphene. *ACS Nano* **5**(2): 805–810.

Kung, H.H., Kung, M.C and Costello, C.K. (2003). Supported Au catalysts for low temperature CO oxidation. *Journal of Catalysis* **216**(1-2): 425–432.

Li, N., Chen, Q.Y., Luo, L.F., Huang, W.X., Luo, M.F., Hu, G.S and Lu, J.Q. (2013). Kinetic study and the effect of particle size on low temperature CO oxidation over Pt/TiO_2 catalysts. *Applied Catalysis B: Environmental* **142**: 523–532.

Li, S., Liu, G., Lian, H., Jia, M., Zhao, G., Jiang, D and Zhang, W. (2008). Low-temperature CO oxidation over supported Pt catalysts prepared by colloid-deposition method. *Catalysis Communications* **9**(6): 1045–1049.

Lin, S.D., Bollinger, M and Vannice, M.A. (1993). Low temperature CO oxidation over Au/TiO2 and Au/SiO2 catalysts. *Catalysis Letters* **17**(3): 245–262.

Liu, C., Li, G., Kauffman, D. R., Pang, G. and Jin, R. (2014). Synthesis of ultrasmall platinum nanoparticles and structural relaxation. *Journal of Colloid and Interface Science* **423**: 123–128.

Liu, L., Zhou, F., Wang, L., Qi, X., Shi, F and Deng, Y. (2010). Low-temperature CO oxidation over supported Pt, Pd catalysts: Particular role of FeOx support for oxygen supply during reactions. *Journal of Catalysis* **274**(1): 1–10.

Lopez, N., Janssens, T.V.W., Clausen, B.S., Xu, Y., Mavrikakis, M., Bligaard, T and Nørskov, J.K. (2004). On the origin of the catalytic activity of gold nanoparticles for low-temperature CO oxidation. *Journal of Catalysis* **223**(1): 232–235.

Meyer, R., Lemire, C., Shaikhutdinov, S. K and Freund, H. J. (2004). Surface chemistry of catalysis by gold. *Gold Bulletin* **37**(1): 72–124.

Moates, F.C., Somani, M., Annamalai, J., Richardson, J.T., Luss, D. and Willson, R.C., 1996. Infrared thermographic screening of combinatorial libraries of heterogeneous catalysts. *Industrial & Engineering Chemistry Research* **35**(12): 4801–4803.

Molina, L.M., Lesarri, A and Alonso, J.A. (2009). New insights on the reaction mechanisms for CO oxidation on Au catalysts. *Chemical Physics Letters* **468**(4-6): 201–204.

Overbury, S. H., Schwartz, V., Mullins, D. R., Yan, W and Dai, S. (2006). Evaluation of the Au size effect: CO oxidation catalyzed by Au/TiO2. *Journal of Catalysis* **241**(1): 56–65.

Rashkeev, S.N., Lupini, A.R., Overbury, S.H., Pennycook, S.J and Pantelides, S.T. (2007). Role of the nanoscale in catalytic CO oxidation by supported Au and Pt nanostructures. *Physical Review B* **76**(3): 035438. DOI:10.1103/physRevB.76.035438.

Remediakis, I.N., Lopez, N and Nørskov, J.K., 2005. CO oxidation on rutile-supported Au nanoparticles. *Angewandte Chemie International Edition* **44**(12): 1824–1826.

Risse, T., Shaikhutdinov, S., Nilius, N., Sterrer, M and Freund, H.J., 2008. Gold supported on thin oxide films: from single atoms to nanoparticles. *Accounts of Chemical Research* **41**(8): 949–956.

Schubert, M.M., Hackenberg, S., Van Veen, A.C., Muhler, M., Plzak, V and Behm, R.J., 2001. CO oxidation over supported gold catalysts—"Inert" and "active" support materials and their role for the oxygen supply during reaction. *Journal of Catalysis* **197**(1): 113–122.

Shaikhutdinov, S.K., Meyer, R., Naschitzki, M., Bäumer, M and Freund, H.J. (2003). Size and support effects for CO adsorption on gold model catalysts. *Catalysis Letters* **86**(4): 211-219.

Somorjai, G. A. (1994). Introduction to Surface Chemistry and Catalysis. John Wiley & Sons, New York.

Strasser, P., Fan, Q., Devenney, M., Weinberg, W.H., Liu, P and Nørskov, J.K. (2003). High throughput experimental and theoretical predictive screening of materials− a comparative study of search strategies for new fuel cell anode catalysts. *The Journal of Physical Chemistry B* **107**(40): 11013–11021.

Zhang, L., Persaud, R and Madey, T. E. (1997). Ultrathin metal films on a metal oxide surface: Growth of Au on TiO_2 (110). *Physical Review B* **56**(16): 10549.